Study of a Numerical Scheme with Transport-Acoustic Operator Splitting on a Staggered Mesh

Ahmad El Halabi[1,5], Pierre Fernier[2,6], Thomas Galie[1,7], Samuel Kokh[3,8], and Khaled Saleh[4,9]

[1] Univ. Paris-Saclay, CEA, Service de Thermo-hydraulique et de Mécanique des Fluides, 91191, Gif-sur-Yvette, France,
[2] Sorbonne Université
[3] Univ. Paris-Saclay, CEA, Service de Génie Logiciel pour la Simulation, 91191, Gif-sur-Yvette, France,
[4] Université de Lyon, CNRS UMR 5208, Université Lyon 1, Institut Camille Jordan, 43 bd 11 novembre 1918; F-69622 Villeurbanne cedex, France
[5] ahmad.elhalabi@cea.fr,
[6] pierrefernier@yahoo.fr
[7] thomas.galie@cea.fr,
[8] samuel.kokh@cea.fr,
[9] saleh@math.univ-lyon1.fr.

Abstract. We present an approximation of the Euler equations by the means of an explicit finite volume method on a staggered grid scheme. The discretization strategy relies on a two-step algorithm that accounts separately for the acoustic and material transport effects in a similar way to the Lagrange-Projection methods.

Keywords: Euler equations, staggered mesh, finite volume methods, operator splitting

1 Introduction

Staggered grid discretizations have been originally designed for the approximation of incompressible flows. Since the seminal work [6], this approach has been extended to compressible models, the main objective being to simulate flows which may be both in highly compressible (large Mach number) and nearly incompressible (low Mach number) regimes. The staggered location of the unknown over the mesh provides for Cartesian meshes a natural mean of evaluation of fluxes and gradients. However, as the original method is not conservative, the computation of shocks can be difficult.

Over the past years many contributions have suggested means to restore conservativity, enhance the stability of the method as well as extensions to unstructured meshes (see [5, 7, 8, 4, 3] and the references therein).

In this study, we present a fully conservative explicit staggered discretization for approximating one-dimensional compressible flows. The method relies on a

separate treatment of acoustic and transport phenomena by means of an operator splitting that shares similarities with the Lagrange-Projection method as in [4], for instance. However one of the main difference of our scheme compared to the latter is the use of a relaxation approach for the linearization of the pressure gradient (see [1] for details). Thus this new scheme follows the ideas developed for the colocated method of [2], our final goal being the simulation of multiphase flows near the incompressible regime on general meshes.

2 Flow equations and acoustic/transport operator splitting approximation

We consider in this work a one-dimensional flow that is governed by the classic compressible Euler equations. We note ρ, u and e respectively the density, velocity and specific internal energy of the fluid. We suppose that the pressure P is given by an Equation Of State (EOS) of the form $P = \mathcal{P}^{eos}(\rho, e)$. The sound velocity c is classically defined by $c^2 = \partial_\rho \mathcal{P}^{eos} + (P/\rho^2)\partial_e \mathcal{P}^{eos}$ and is supposed to be real-valued. If $E = e + u^2/2$ denotes the specific total energy, the equation of motion reads in a one-dimensional setting

$$\rho_t + (\rho u)_x = 0, \qquad (\rho u)_t + (\rho u^2 + P)_x = 0, \qquad (\rho E)_t + (\rho E u + P u)_x = 0. \tag{1}$$

Following [2], we remark that smooth solutions of (1) verify

$$\begin{aligned} \rho_t &+ \rho u_x &&+ u\rho_x &&= 0, &\text{(2a)}\\ (\rho u)_t &+ \rho u u_x + P_x &&+ u(\rho u)_x &&= 0, &\text{(2b)}\\ (\rho E)_t &+ \rho E u_x + (Pu)_x &&+ u(\rho E)_x &&= 0. &\text{(2c)} \end{aligned}$$

This suggests to consider the subsystems

$$\rho_t + \rho u_x = 0, \quad (\rho u)_t + \rho u u_x + P_x = 0, \quad (\rho E)_t + \rho E u_x + (Pu)_x = 0 \tag{3}$$

and

$$\rho_t + u\rho_x = 0, \qquad (\rho u)_t + u(\rho u)_x = 0 \qquad (\rho E)_t + u(\rho E)_x = 0. \tag{4}$$

As in [2], we propose to approximate the solutions of (1) by successively approximating the solution of (3) and (4). Before going any further, let us briefly recall properties of the subsystems (3) and (4). The acoustic system (3) reads equivalently

$$\rho\,(1/\rho)_t - u_x = 0, \qquad \rho u_t + P_x = 0, \qquad \rho E_t + (Pu)_x = 0, \tag{5}$$

and its associated Jacobian matrix possesses three eigenvalues $(-c, 0, c)$, so that it is strictly hyperbolic. The waves associated with the characteristic velocities $\pm c$ are genuinely nonlinear while the stationary wave is linearly degenerate. The transport system (4) is hyperbolic as it has diagonal form with u as triple characteristic velocity.

3 Staggered discretization

We consider a discretization of the real line into (primal) cells $K_i = (x_{i-1/2}, x_{i+1/2})$ with $i \in \mathbb{Z}$ and a series of instant $t^{n+1} = t^n + \delta t^n$ for $n \in \mathbb{N}$, where $\Delta x_i = x_{i+1/2} - x_{i-1/2} > 0$ is a space step and $\delta t^n > 0$ is the time step. The intervals $D_{i+1/2} = (x_i, x_{i+1})$ are referred to as dual cells, with $x_i = (x_{i+1/2}+x_{i-1/2})/2$ and $\Delta x_{i+1/2} = x_{i+1} - x_i$. For any fluid parameter b, we note b_i^n and $b_{i+1/2}^n$ respective approximations of $\frac{1}{\Delta x_i}\int_{K_i} b(x,t^n)\mathrm{d}x$ and $\frac{1}{\Delta x_{i+1/2}}\int_{D_{i+1/2}} b(x,t^n)\mathrm{d}x$. If the vector $\mathcal{U}^n = \left(\rho_i^n, (\rho u)_{i+1/2}^n, (\rho E)_i^n\right)^T$ denotes a discrete approximate solution of (1) at instant t^n, the overall numerical scheme will first yield an updated value $\widetilde{\mathcal{U}}$ by integrating the acoustic system (3). Then by approximating the solution of the transport system (4) we will obtain the updated fluid parameters $\mathcal{U}^{n+1}$ at t^{n+1}. In the following, we will note $\lambda_k^n = \delta t^n/\Delta x_k$, for $n > 0$ and $k \in \mathbb{Z}/2$.

3.1 Approximation of the acoustic subsystem

Using a similar strategy as in [2], we consider a Suliciu-type relaxation approximation of (5) that reads

$$r\left(1/\rho\right)_t - u_x = 0, \qquad ru_t + \pi_x = 0, \qquad rE_t + (\pi u)_x = 0, \quad (6a_\nu)$$

$$r_t = \nu(\rho - r), \quad r\pi_t + a^2 u_x = \nu(P - \pi), \quad (6b_\nu)$$

where $a > 0$ is an approximation of ρc that needs to be chosen large enough in order to ensure stability. More precisely, a must satisfy Whitham's condition which reads $a^2 > (\rho c)^2$ in order for system (6) to be a viscous approximation of system (3). Formally by considering system (6) in the limit $\nu \to \infty$, one retrieves the acoustic system (5). In practice, the regime $\nu \to \infty$ is obtained at each time step t^n by classically enforcing $r_i^n = \rho_i^n$ and $\pi_i^n = \mathcal{P}^{eos}(\rho_i^n, e_i^n)$. Therefore, the equation on r just expresses the fact that the density is constant over the acoustic step while the equation on π is used as a linearization of the pressure gradient in the momentum equation. We discretize (6) with the following update formula

$$\rho_i^n\left(1/\widetilde{\rho}_i - 1/\rho_i^n\right) - \lambda_i^n\left(u_{i+1/2}^* - u_{i-1/2}^*\right) = 0, \quad (7a)$$

$$\rho_{i+1/2}^n\left(\widetilde{u}_{i+1/2} - u_{i+1/2}^n\right) + \lambda_{i+1/2}^n\left(\widetilde{\pi}_{i+1} - \widetilde{\pi}_i\right) = 0, \quad (7b)$$

$$\rho_i^n\left(\widetilde{E}_i - E_i^n\right) + \lambda_i^n\left(\widetilde{\pi}_{i+1/2}^* u_{i+1/2}^* - \widetilde{\pi}_{i-1/2}^* u_{i-1/2}^*\right) = 0, \quad (7c)$$

$$\rho_i^n\left(\widetilde{\pi}_i - \pi_i^n\right) + a_i^2\lambda_i^n\left(u_{i+1/2}^* - u_{i-1/2}^*\right) = 0, \quad (7d)$$

where $a_i = \rho_i^n c_i^n$ and

$$u_{i+1/2}^* = u_{i+1/2}^n - \frac{1}{2a_{i+1/2}}\left(\pi_{i+1}^n - \pi_i^n\right) \quad \text{with } a_{i+1/2} = \rho_{i+1/2}^n c_{i+1/2}^n, \quad (8a)$$

$$\widetilde{\pi}_{i+1/2}^* = \theta_{i+1/2}\widetilde{\pi}_i + \left(1 - \theta_{i+1/2}\right)\widetilde{\pi}_{i+1} \quad \text{with } \theta_{i+1/2} = \frac{1}{1 + \frac{\rho_i^n \Delta x_i}{\rho_{i+1}^n \Delta x_{i+1}}}. \quad (8b)$$

One can notice that $0 < \theta_{i+1/2} < 1,\ \forall i \in \mathbb{Z}$, so that the pressure at face $\widetilde{\pi}^*_{i+1/2}$ is a convex combination of the corresponding left and right relaxation pressures. The variables $\rho^n_{i+1/2}, c^n_{i+1/2}$ and E^n_i are defined as follow :

$$\varphi^n_{i+1/2} = \frac{\Delta x_i \varphi^n_i + \Delta x_{i+1}\varphi^n_{i+1}}{2\Delta x_{i+1/2}}, \quad \text{for } \varphi \in \{\rho, c\}\,, \tag{9a}$$

$$E^n_i = e^n_i + \frac{1}{2}\left[\left(u^n_{i-1/2}\right)^2/2 + \left(u^n_{i+1/2}\right)^2/2\right]. \tag{9b}$$

3.2 Approximation of the transport subsystem

For more convenience, we will note in the following $\Delta\varphi^*_i = \varphi^*_{i+1/2} - \varphi^*_{i-1/2}$, for $\varphi \in \{u, \pi u\}$ and $\Delta\varphi^*_{i+1/2} = \varphi^*_{i+1} - \varphi^*_i$ for $\varphi \in \{\pi, u\}$ and $i \in \mathbb{Z}$. The discretization of the transport system (4) is performed following [2], more precisely we use the fact that $u\varphi_x = (u\varphi)_x - \varphi u_x$ for $\varphi \in \{\rho, \rho u, \rho E\}$. Thus, by writting $\delta\mathcal{U}^{n+1} = \mathcal{U}^{n+1} - \widetilde{\mathcal{U}}$, the update during the transport step writes

$$\delta\rho^{n+1}_i + \lambda^n_i\left(F_{i+1/2} - F_{i-1/2} - \widetilde{\rho}_i\Delta u^*_i\right) = 0, \tag{10a}$$

$$\delta(\rho u)^{n+1}_{i+1/2} + \lambda^n_{i+1/2}\left(F_{i+1}\widetilde{u}^{up}_{i+1} - F_i\widetilde{u}^{up}_i - \widetilde{(\rho u)}_{i+1/2}\Delta u^*_{i+1/2}\right) = 0, \tag{10b}$$

$$\delta\left(\rho E\right)^{n+1}_i + \lambda^n_i\left(F_{i+1/2}\widetilde{E}^{up}_{i+1/2} - F_{i-1/2}\widetilde{E}^{up}_{i-1/2} - \widetilde{(\rho E)}_i\Delta u^*_i\right) = 0. \tag{10c}$$

The numerical mass flux $F_{i+1/2}$ and total energy $\widetilde{E}^{up}_{i+1/2}$ are evaluated thanks to the classical upwind flux, more precisely

$$F_{i+1/2} = \widetilde{\rho}^{up}_{i+1/2}u^*_{i+1/2}, \quad \text{with} \quad (\widetilde{\rho}, \widetilde{E})^{up}_{i+1/2} = \begin{cases} (\widetilde{\rho}, \widetilde{E})_i, & \text{if } u^*_{i+1/2} > 0, \\ (\widetilde{\rho}, \widetilde{E})_{i+1}, & \text{otherwise.} \end{cases}$$

In (10b), the momentum fluxes F_i are evaluated using an upwind procedure proposed in [8] that can be expressed as follow :

$$\widetilde{u}^{up}_i = \begin{cases} \widetilde{u}_{i-1/2}, & \text{if } F_i > 0 \\ \widetilde{u}_{i+1/2}, & \text{otherwise.} \end{cases} \quad \text{with } F_i = \frac{\Delta x_{i-1/2}F_{i-1/2} + \Delta x_{i+1/2}F_{i+1/2}}{2\Delta x_i}.$$

3.3 Overall scheme

If we set $\widetilde{\rho}_{i+1/2} = \rho^n_{i+1/2}/\left(1 + \lambda^n_{i+1/2}\Delta u^*_{i+1/2}\right)$, the overall update of the conservative variable by the Staggered-Lagrange-Projection (SLP) takes the form of the following conservative scheme

$$\rho^{n+1}_i = \rho^n_i - \lambda^n_i\left(F_{i+1/2} - F_{i-1/2}\right), \tag{11a}$$

$$(\rho u)^{n+1}_{i+1/2} = (\rho u)^n_{i+1/2} - \lambda^n_{i+1/2}\left(F_{i+1}\widetilde{u}^{up}_{i+1} - F_i\widetilde{u}^{up}_i + \Delta\widetilde{\pi}_{i+1/2}\right), \tag{11b}$$

$$(\rho E)^{n+1}_i = (\rho E)^n_i - \lambda^n_i\left(F_{i+1/2}\widetilde{E}^{up}_{i+1/2} - F_{i-1/2}\widetilde{E}^{up}_{i-1/2} + \Delta\left(\widetilde{\pi}^* u^*\right)_i\right). \tag{11c}$$

Given the update value of E_i^{n+1} and $u_{i+1/2}^{n+1}$ obtained by (11), the updated value e_i^{n+1} of the internal energy is obtained thanks to (9b). The time step is set according to the relation

$$\delta t = K \min\left(\delta t_{ac}, \delta t_{tr}\right), \quad K \in (0,1), \tag{12}$$

where δt_{ac} and δt_{tr} are given by

$$\delta t_{ac} = \min_{i\in\mathbb{Z}} \left(\frac{\Delta x_i}{(\Delta u_i^*)^-} \right) \quad \text{and} \quad \delta t_{tr} = \min_{i\in\mathbb{Z}} \left(\frac{\Delta x_i}{\left(u_{i+1/2}^*\right)^+ + \left(-u_{i-1/2}^*\right)^+} \right)$$

with $b^- = -\min(b,0)$ and $b^+ = \max(b,0)$. The time step δt_{ac} ensures the positivity of $\widetilde{\rho}_i$ in (7a) while δt_{tr} ensures the positivity of ρ_i^{n+1} in (11a). One can show the following proposition.

Proposition 1. *The SLP scheme* (11) *is conservative with respect to the density, momentum, total energy and under the condition* (12) *it preserves the positivity of the density.*

A proof of this proposition can be obtained following similar lines as in [2].

4 Numerical Results

We now test our numerical SLP scheme against classical tests of the literature and also display comparison with the MAC scheme presented in [8]. In the following, the fluid is supposed to be governed by the Perfect Gas EOS defined by $\mathcal{P}^{eos}(\rho, e) = (\gamma - 1)\rho e$, with $\gamma = 1.4$. All tests have been running with constant value $K = 0.1$ in the stability condition (12). Initial conditions of the first two tests are detailed in [10] and the third one in [9, problem case 3].

Toro test 4 We propose to test the new SLP scheme against a first classical Riemann problem. This test represents the collision of two strong right and left shocks and consists of a left facing shock, a right travelling contact discontinuity and a right travelling shock wave. The computation was performed using a 500-cell mesh. We can see in Figure 1 that the SLP scheme succeeds in capturing the right discontinuities while the MAC scheme suffers an overshoot near the shock.

Toro test 5 We now turn to a second classical Riemann problem. For this test, we also used a 500-cell grid. The test consists in a left rarefaction wave, a contact discontinuity and a strong right shock. Figure 2 displays a comparison between the SLP scheme and the MAC scheme. One can observe spurious oscillations in the MAC scheme in the intermediate state where the velocity vanishes and of maximal amplitude near the right shock. This behavior of the explicit MAC

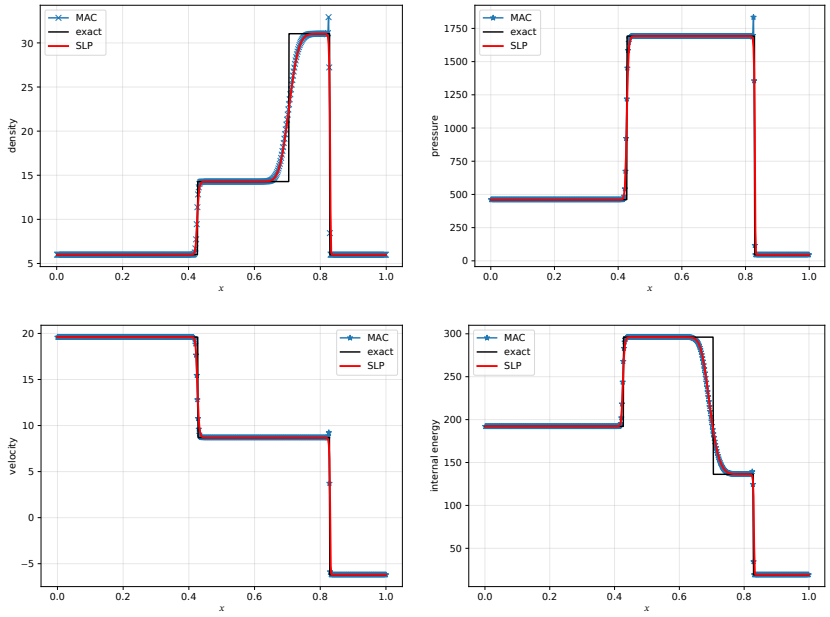

Fig. 1. Results obtained for Toro test 4 at instant $t = 0.035$.

scheme is already known and is due to a lack of numerical dissipation in the momemtum equation when the velocity vanishes, as already pointed out in [8]. The SLP scheme does not suffer of such oscillations, mostly thanks to the extra diffusive term in the face velocity (8a).

Two-dimensional Riemann problem Using a directional splitting, the SLP scheme can be extended to multi-dimensional problems approximated over a Cartesian grid. We consider the two-dimensional Riemann problem of case 3 studied in [9] and performed using a 400×400-cell regular mesh. Results for both schemes are displayed in Figure 3. Spurious oscillations appear for the MAC scheme mostly in the zero-velocity region of the test, which is caused by a lack of numerical dissipation as previously discussed. On the other hand, the new SLP scheme does not exhibit such behavior and presents good agreement with results shown in [9].

5 Conclusion

We proposed a fully conservative discretization of the compressible Euler equations over a staggered mesh using an explicit acoustic/transport operator splitting approach. The method shows promising results on both one-dimensional and two-dimensional tests. Further works also include a more thorough study of the stability properties of the scheme and the extension to unstructured meshes.

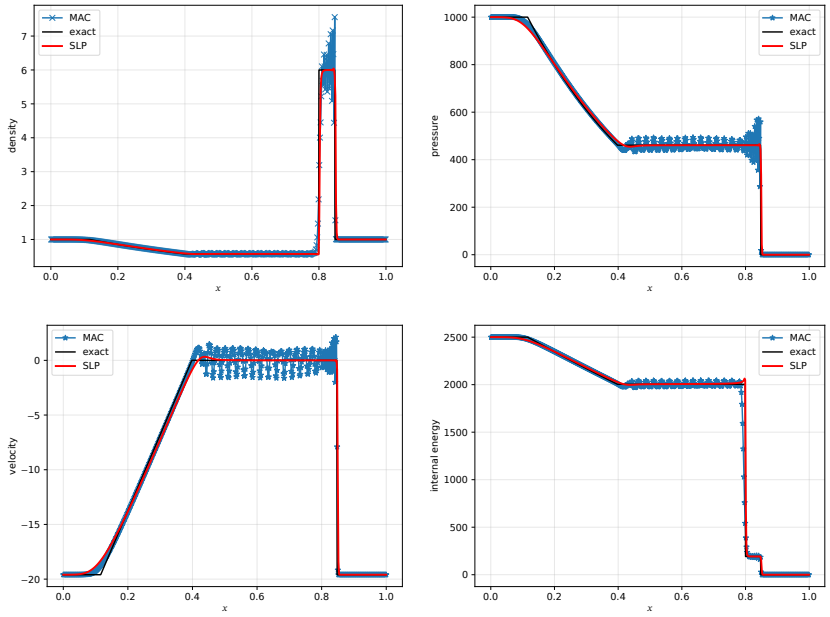

Fig. 2. Results obtained for the Toro test 5 at instant $t = 0.012$.

References

1. F. Bouchut. *Nonlinear Stability of Finite Volume Methods for Hyperbolic Conservation Laws*, pages pp. 33–36. Birkhäuser Basel, 2004.
2. C. Chalons, M. Girardin, and S. Kokh. An all-regime Lagrange-Projection like scheme for the gas dynamics equations on unstructured meshes. *Comm. in Comp. Phys.*, 20(1):pp. 188–233, 2016.
3. G. Dakin, B. Després, and S. Jaouen. High-order staggered schemes for compressible hydrodynamics. weak consistency and numerical validation. *JCP*, 376:pp. 339–364, jan 2019.
4. G. Dakin and H. Jourdren. High-order accurate lagrange-remap hydrodynamic schemes on staggered cartesian grids. *Comptes Rendus Mathématique*, 354(2):pp. 211–217, feb 2016.
5. T. Goudon, J. Llobell, and S. Minjeaud. A staggered scheme for the euler equations. In *Springer Proceedings in Mathematics & Statistics*, pages pp. 91–99. Springer International Publishing, 2017.
6. F Harlow and A Amsden. A numerical fluid dynamics calculation method for all flow speeds. *JCP*, 8(2):pp. 197–213, oct 1971.
7. R. Herbin, W. Kheriji, and J.-C. Latché. Staggered schemes for all speed flows. *ESAIM: Proceedings*, 35:pp. 122–150, mar 2012.
8. R. Herbin, J.-C Latché, and T. T. Nguyen. Consistent segregated staggered schemes with explicit steps for the isentropic and full Euler equations. *ESAIM: Mathematical Modelling and Numerical Analysis*, 52(3):pp. 893–944, 2018.

9. R. Liska and B. Wendroff. Comparison of several difference schemes on 1d and 2d test problems for the euler equations. *SIAM Journal on Scientific Computing*, 25(3):pp. 995–1017, 2003.
10. Eleuterio F. Toro. *Riemann Solvers and Numerical Methods for Fluid Dynamics*, pages pp. 404–405. Springer Berlin Heidelberg, 2009.

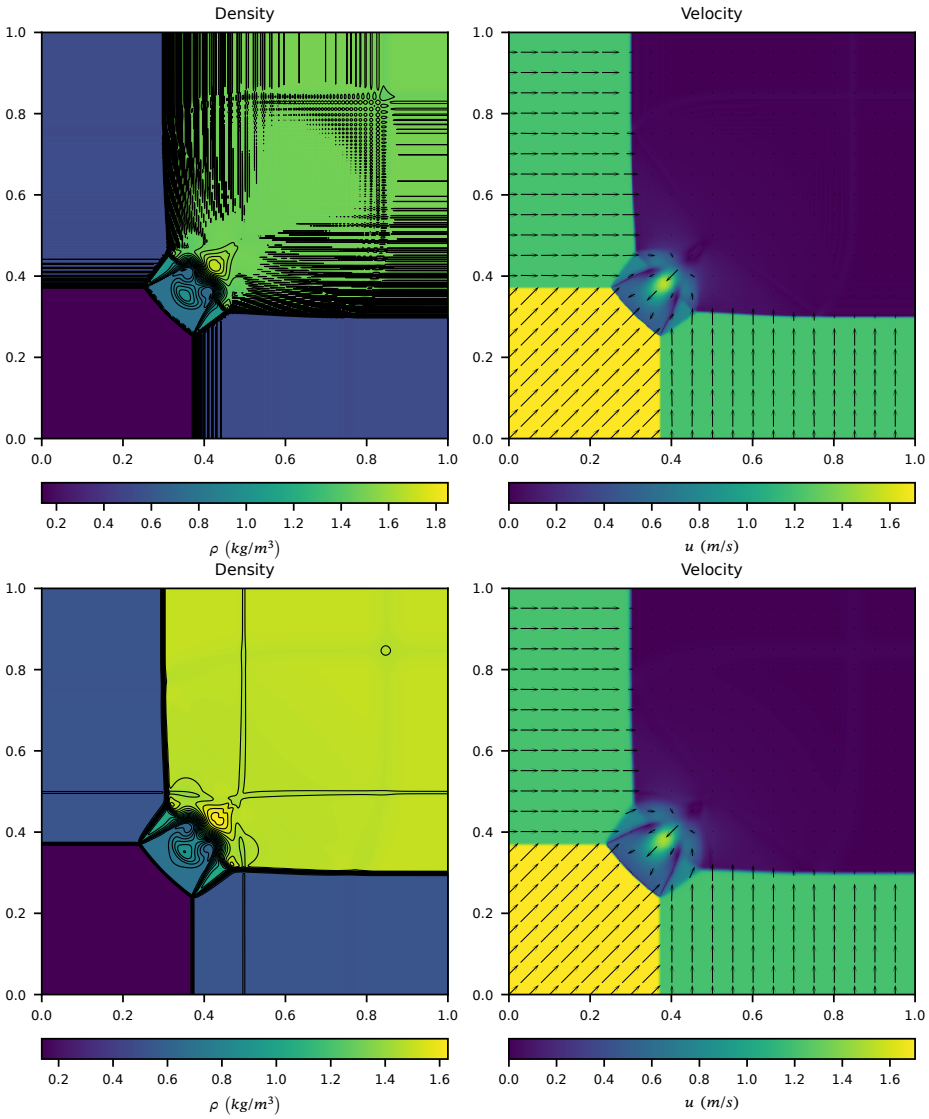

Fig. 3. Two-dimensional Riemann problem: results for the MAC (above) and the SLP schemes (below) at instant $t = 0.3$